JMEPEG (2001) 10:629–634

Iridium-Based Refractory Superalloys by Pulse Electric Current Sintering Process: Part 1. Elemental Powder

C. Huang, Y. Yamabe-Mitarai, and H. Harada

(Submitted 21 May 2001; in revised form 24 July 2001)

Pulse electric current sintering (PECS) was tried as a novel powder metallurgy (PM) process for five Ir-based elemental powder mixtures. Sintering was carried out at 1800 °C for 4 h for all the samples. Specimens with a relative density, more than 90% theoretical density, were obtained after sintering. More than two phases were found; however, a single phase ($L1_2$ or B2) was expected, according to the phase diagram. The densification mechanism is discussed briefly, and remaining problems are presented.

Keywords density, elemental powder, Ir-based refractory superalloy, microstructure, phase, pore, powder metallurgy, pulse electric current sintering

1. Introduction

In an effort to meet the increasing demand for high-temperature alloys, many efforts have been made to develop new materials that perform better than Ni-based superalloys. The platinum group metals, by virtue of their excellent corrosion resistance and high-melting points, are well suited to a wide range of high-temperature applications.[1] Yamabe-Mitarai *et al.*[2] has developed a new series of alloys called "refractory superalloys" that use metals from the platinum group. The experimental results show that Ir-based superalloys also have a fcc/$L1_2$ two-phase coherent structure that is similar to that of Ni-based superalloys, yet with a higher melting temperature and improved high-temperature strength.

However, the usual fabrication method of arc melting, which has been used for these alloys until now, has disadvantages because it leads to a brittle structure, poor workability,[1] and a heterogeneous microstructure. Even after the samples were heat treated, they usually broke when the samples were cut with an electric discharge machine or when they were placed on tensile test equipment. The development of Ni-based superalloys by the powder metallurgy (PM) process that have more improved properties than superalloys by conventional methods give us the inspiration to try to improve the performance of Ir-based refractory superalloys using the PM process. Pulse electric current sintering (PECS) is a new process for powder densification in the PM area. Compared with conventional sintering, PECS has an advantage by which the current can cross the powder compact directly to generate interparticle plasma that activates the particle surface[3] and causes the sintering to progress in a short time.

In a previous study, Ir and Nb elemental-powder mixtures, with a composition of Ir-25 at.% Nb for obtaining the $L1_2$ single phase, were tried using sintering times from several minutes to 2 h by the PECS process. However, Nb segregated, and the alloying process did not finish perfectly.[4] As is well known, the liquid phase that forms during sintering can drastically increase the densification rate; moreover, when a low-melting-temperature powder is melted, a large heat of formation is introduced that results in a remarkable increase in the temperature of the powder mixture that is being sintered.[5] Hideki Hosoda *et al.*[6] succeeded in obtaining an Ir-50 at.% Al alloy using hot press (HP) by using a large heat of formation from Al. In the present work, five kinds of powder mixture were investigated. 1 at.% Al or 1 at.% Ni was added into Ir-24 at.% Nb or Ir-25 at.% Nb powder mixtures in order to obtain a large heat of formation. For comparison, Ir-25 at.% Nb was tried again. Ir-25 at.% Ti and Ir-50 at.% Al, which have a low-melting-point constituent, were studied.

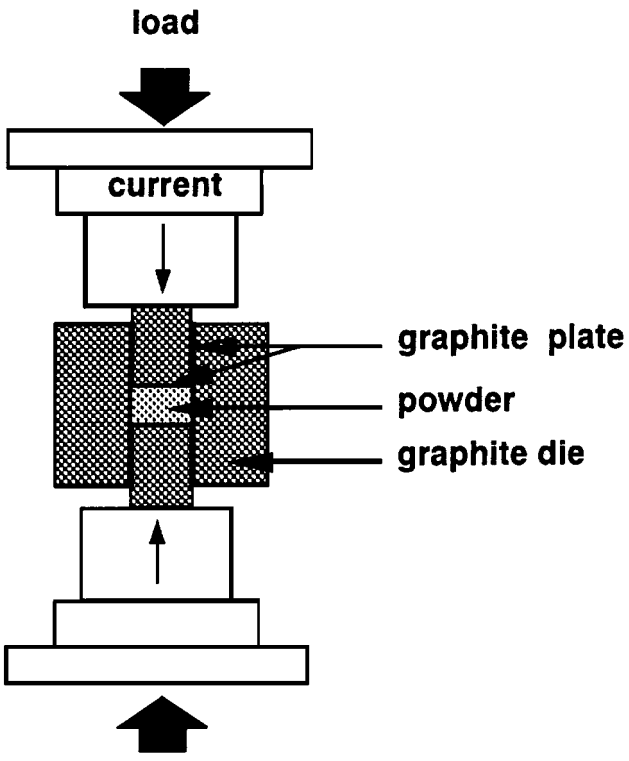

Fig. 1 Schematic diagram of PECS process

C. Huang, Y. Yamabe-Mitarai, and **H. Harada,** National Institute for Materials Science (NIMS), Tsukuba, Ibaraki 305-0047, Japan. Contact e-mail: huang.chen@nims.go.jp.

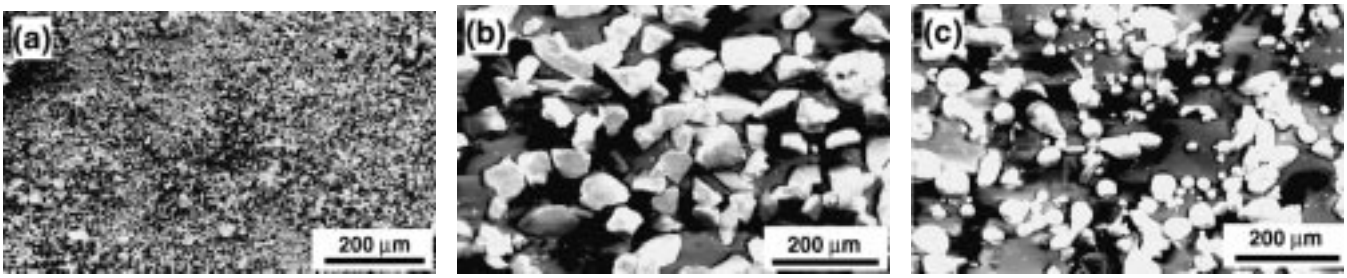

Fig. 2 Powder-size distribution under SEM observation: (**a**) Ir, (**b**) Nb, and (**c**) Al

Table 1 The composition, powder size, and sintering conditions of investigated samples

Alloy composition (at.%)	Powder size (mesh)	Sintering condition: initial heating rate
Ir:Nb = 75:25		2 min 8 min 2 min 572 °C → 600 °C → 1750 °C → 1800 °C
Ir:Nb:Al = 75:24:1	Al: −200	2 min 1 min 20 min 7 min 2 min 572 °C → 600 °C → 640 °C → 680 °C → 1750 °C → 1800 °C
Ir:Nb:Ni = 74:25:1	Ni: −325	2 min 6 min 25 min 2 min 2 min 572 °C → 600 °C → 1420 °C → 1470 °C → 1750 °C → 1800 °C
Ir:Al = 50:50	Al: −200	2 min 1 min 20 min 7 min 2 min 572 °C → 600 °C → 640 °C → 680 °C → 1750 °C → 1800 °C
Ir:Ti = 75:25	Ti: −100	2 min 7 min 25 min 1 min 2 min 572 °C → 600 °C → 1650 °C → 1700 °C → 1750 °C → 1800 °C

Table 2 Calculated and actual densities

Alloy (at.%)	Corrected composition (at.%)	Theoretical max. density (g/cm^3)	Actual density (g/cm^3)	Relatively density (%TD)
Ir-25% Nb		18.21	17.28	94.89
Ir-24% Nb-1% Al(a)	Ir-18.2% Nb-1.9% Al	19.04	18.55	97.43
Ir-25% Nb-1% Ni(a)	Ir-20.9% Nb-0.5% Ni	19.15	17.51	91.44
Ir-50% Al		11.81	11.30	95.68
Ir-25% Ti(a)	Ir-25.3% Ti	17.31	16.67	96.30

(a) Some metals were squeezed out of the graphite die when 1800 °C was reached

2. Experimental Procedure

Five elemental-powder mixture samples of 5 g each were prepared. The mixtures were poured into a plastic bottle and then placed on a milling machine with one direction rotation and milled for 24 h. After that, the powders were put into a graphite die and placed into the PECS furnace. The schematic diagram of the PECS process is shown in Fig. 1. Sintering was carried out in a vacuum of $\sim 0.5 \times 10^{-2}$ torr and with a load of about 40 MPa. The samples were heated to 1800 °C with different heat rates, which were slower around the melting temperature of a low-melting-point element and were then kept at 1800 °C for 4 h. (The temperature here was measured by optical pyrometry at a chosen point of the die surface.) The computer connected to the PECS machine simultaneously reported the displacement and temperature of the powder compact as well as the pressure on it. The composition of the samples investigated, powder-particle size, and initial heat rate are listed in Table 1. The powder sizes of Ir and Nb were observed under a scanning electron microsope (SEM). The results for Ir and Nb are shown in Fig. 2. For comparison, the size of Al was also presented.

The specimens (about 15 mm in diameter and 1 mm or so in thickness) taken out of the graphite die were ground to remove the carbon contamination on the surface. The thickness and diameter were measured by micrometer to calculate the actual density. The specimens were then cut into three parts, a large one and two smaller ones. The large one was used for x-ray diffraction analysis to determine the phase structure. The two smaller ones were embedded together in one resin block with different observation faces (one with a specimen surface and the other with a cross section) that were polished and etched with a solution of 5% HCl in ethyl alcohol for observation with an optical microscope and an SEM. The compositions of the constituent phase were measured by energy-dispersive analysis x-ray spectroscopy (EDX). The actual composition of some of the specimens was analyzed by the fluorescence x-ray method.

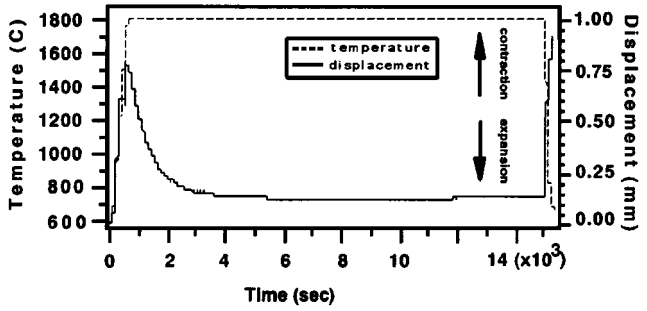

(**a**)

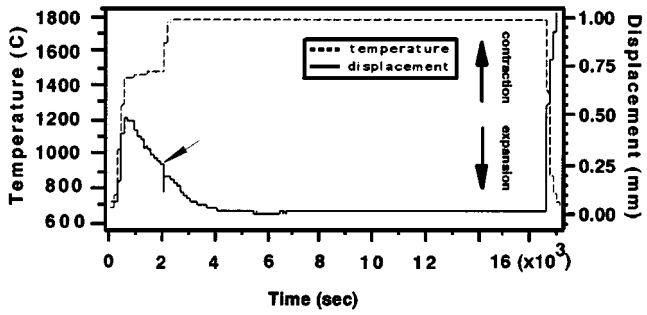

(**b**)

Fig. 3 Representative temperature and displacement curve during sintering (**a**) Ir-25% Nb and (**b**) Ir- 24% Nb-1% Al

3. Results and Discussion

3.1 Sintering Behavior

Figure 3 shows the representative temperature and displacement curves. During sintering, along with the change of temperature, the powder compact initially contracted and then expanded. Similar behavior was shown for all five samples during sintering. In the beginning, the powder compacts contracted for more than 10 min and then expanded as the temperature increased. For some time after 1800 °C was reached, the powder compact quit expanding and became stable until it cooled. The contraction at the beginning of sintering is attributed to the gas elimination within powders as the temperature began to increase.

3.2 Density

The theoretical (maximum sintered) densities of the composite powder were calculated using a simple method of mixtures formula:

$$\rho = 1/(C_a/\rho_a + C_b/\rho_b + C_c/\rho_c) \qquad \text{(Eq 1)}$$

where ρ is the theoretical composite density; c is the concentration in weight percent of components a, b, and c; and ρ_a, ρ_b, and ρ_c are component densities.[7] Theoretical and actual densities are given in Table 2. During sintering, some melted metals of Ir-25% Ti, Ir-24% Nb-1% Al, and Ir-25% Nb-1% Ni (noted in Table 2) were squeezed out of the graphite die just when the temperature of 1800 °C was reached. The location of the arrow in Fig. 3(b) shows the point where the molten metals went out. It was supposed to be the reason for heterogeneous melting within powder compact. The sudden change of displacement can be seen very clearly in Fig. 3(b). Also, molten metals attaching on the surface of the graphite die were found after sintering. The compositions in the lost metals were heterogeneous. From the results of fluorescence x-ray analysis for the remaining specimens, there was less Nb in Ir-24 at.% Nb-1 at.% Al and Ir-25 at.% Nb-1 at.% Ni than there was in the nominal composition, and the composition of Ir-25 at.% Ti did not change much. The theoretical density of the three samples was calculated according to the corrected content, which is also shown in Table 2.

3.3 Microstructure

There were no distinct differences between the surface and section in the microstructure of the specimen. The representative micrographs are shown in Fig. 4, and x-ray analysis results are shown in Fig. 5. Pores along grain boundaries as well as inside the grains could be observed quite easily in all samples. However, the distribution of the pores according to size was different. In Ir-25% Nb, Ir-24% Nb-1% Al, and Ir-25% Nb-1% Ni, besides many small pores, many large irregular pores were observed. However, only fine round pores existed in Ir-50% Al. For Ir-25% Ti, in addition to a few big pores, small round pores were dominant. One thing that should be noted is that many small pores existed in all the samples. From the morphologies of the powder, the powder pattern of Ir and Ni was porous, and the others were particulate. Maybe porous powder was the reason for many small pores remaining in the sintered samples. More small pores found in Ir-25% Nb-1% Ni than Ir-25% Nb and Ir-24% Nb-1% Al gave a support, which meant porous powders of Ni increase the amount of small pores.

Judging from phase diagrams, only a single phase, B2 (IrAl) in Ir-50% Al and $L1_2$ (Ir_3Nb or Ir_3Ti) in the other ones, was expected in these samples; however, second phases and even a third phase were detected on x-ray curves (Fig. 5) and microstructure.

One phase ($L1_2$) should form in Ir-25 at.% Nb, Ir-24 at.% Nb-1 at.% Al, and Ir-25 at.% Nb-1 at.% Ni; however, the fcc peak emerged on x-ray results. For Ir-24 at.% Nb-1 at.% Al, Nb was also detected. On the enlarged picture of Fig. 4(f), some of the fcc/$L1_2$ area was found to have a coherent structure. This contributed to the metal loss, which changed the real composition and shifted the composition to the fcc/$L1_2$ two-phase region. Powder mixing was also a problem. By means of EDX, the content of Nb in the area near the big holes was greater than that in the other area. This proved that powder had not been mixed well. Inside the powder compact, some parts were Ir-rich, and some were Nb-rich. The overall microstructures of the three samples looked similar to each other in that two morphologies with distinguishable borders could be seen clearly (Fig. 4c, d, and e). In the area around the big holes, the grain boundary and twins were obvious, and small pores were less so; however, no twins were found in the other area, which had more small pores. The main difference among the three specimens was that there were fewer pores in Ir-25% Nb-1% Al than there were in Ir-25% Nb, and there were more small pores in Ir-25% Nb-1% Ni, which is shown in Fig. 6. Compared

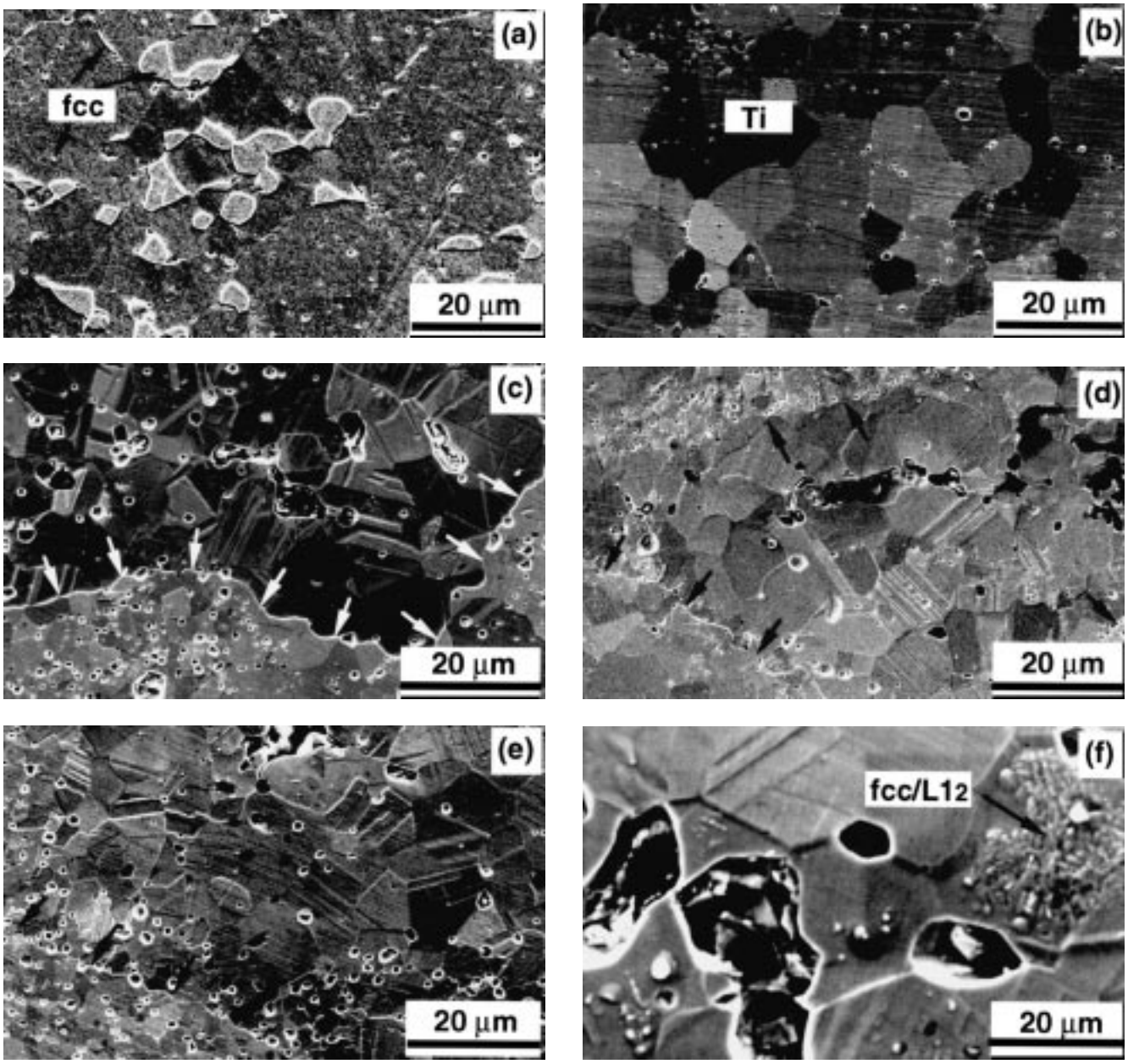

Fig. 4 The SEM microstructures of (**a**) Ir-50% Al, (**b**) Ir-25% Ti, (**c**) Ir-25% Nb, (**d**) Ir-24% Nb-1% Al, (**e**) Ir-25% Nb-1% Ni, and (**f**) enlarged picture of Ir-25% Nb

with the previous studies, the sintering process was improved by extending sintering time to 4 h. With the exception of Ir-24% Nb-1% Al, in which some Nb was found, no pure element was detected in the other two samples. The introduction of Al with a much lower melting temperature than 1800 °C affected the elimination of pores; however, porous Ni powder with a higher melting temperature than Al increased the number of small pores.

For Ir-50% Al, in addition to a matrix phase B2, a fcc phase was found. On the microstructure, an fcc phase with bright contrast was observed in some parts of the specimen. Some of the fcc phase was spherelike, and some was eutectic in structure. By means of EDX, the fcc phase contained ~15 at.% Al. The appearance of an fcc phase was explained by Hosoda *et al.*[6] as the reason of B2 narrow phase region or extremely low diffusivity of Al in Ir. Compared with the alloy fabricated by HP in Hosoda's results, the distribution of fcc in a matrix phase B2 here was heterogeneous. This contributed to the problem that powders were not mixed well. The fcc phase was likely to appear on the Ir-rich area.

On x-ray curves of Ir-25% Ti, Ti was found in addition to the $L1_2$ phase, indicating that some Ti still remained after sintering, which was confirmed by microstructure observation (Fig. 4b). Some Ti even retained round particles, although the particles had already broken into small pieces inside.

The details are summarized in Table 3.

3.4 Densification Mechanism

During the sintering, two processes occurred simultaneously: densification and coarsening (grain growth). The main mechanism of densification could be divided into two types according to whether a liquid phase was forming during the sintering: solid-state diffusion and liquid-phase sintering. On the basis of the melting temperature of pure metal, except in the case of Ir-25% Nb, a liquid phase formed during sintering in the other samples because they had one constituent with a low melting temperature (the melting temperature of Al, Ni, and Ti is 660, 1453, and 1680 °C, respectively, lower than the sintering temperature of 1800 °C).

For Ir-50 at.% Al, the predominant mechanism was liquid-phase sintering because enough Al was included. It was also confirmed from microstructure that there were small round pores and a coarse structure with large grains. For Ir-25 at.% Ti, although the content of Ti was large, the liquid phase did not spread thoroughly through the powders. In the microstructure, there was a lack of uniformity in the distribution of grain according to size. In the area around the remaining Ti, the grain size was large, some even reaching about 40 μm, which means liquid-phase sintering had an effect here; however, in another area, the grain size was quite small. This was attributed to the large difference in the Ir and Ti powder size and also to the low diffusivity of Ti in Ir. For Ir-24% Nb-1% Al and Ir-25% Nb-1% Ni, the main densification force was still solid-state diffusion. 1 at.% Al and Ni could not form enough liquid phases to wet the entire solid particle. The difference of size and shape of the grain among Ir-24% Nb-1% Al, Ir-25% Nb-1% Ni, and Ir-25 at.% Nb could not be found in the microstructure.

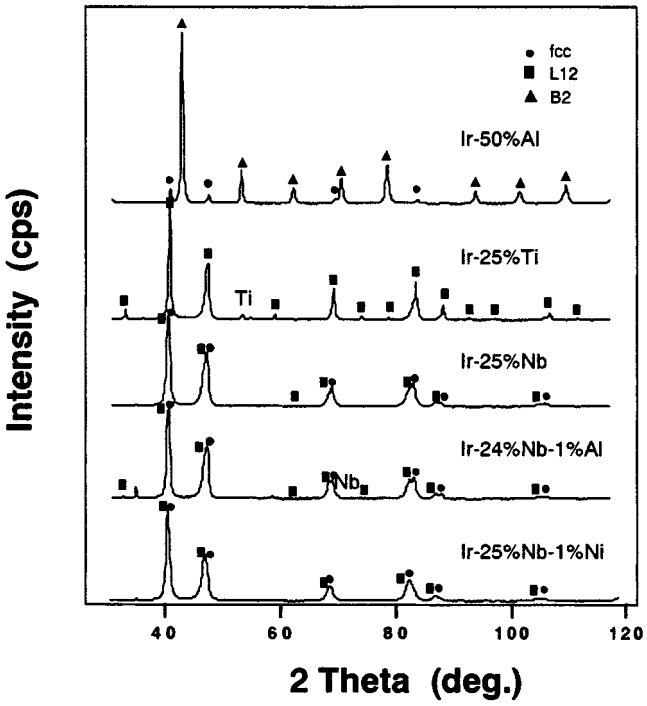

Fig. 5 The XRD pattern of sintered samples

3.5 Problems and Future Work

From the results mentioned previously, the alloying of the PECS process for Ir-based elemental powder mixtures was almost finished. However, some problems remained. The main problems are as follows. (1) Metal is lost during sintering, which changes the composition of the alloys. (2) Pores exist. It is generally accepted that the mechanical properties of powder-metallurgy materials are governed by their remnant porosities. Approximate exponential decays of mechanical properties are caused by linear increases in the volume fractions of pores.[8] (3) The heterogeneous structure forms after sintering, which also decreases the mechanical properties. Although we believed that the microstructure could be improved with the PM process, in this instance, it was not.

The fact that the powder size and shape are not suitable is one of the reasons. The PECS has a special advantage for ultrafine powder, such as several microns, in short-time sintering. However, the finest powder used here was Ni, which is still 45 μm. Moreover, the sizes of the powder were quite different, as shown in Fig. 2. This increased the segregation possibility of each metal. In addition, the powder shape also affected the number of remaining pores. It seemed that porous powder would increase the number of small pores in Ir-based alloys from PECS. Another reason is the milling problem. It is difficult to mill small amounts of powder mixtures (5 g was used in this study) well. Large differences in powder size and differences in the density of Ir (22.42 g/cm^3) and other metals (the lightest was Al with 2.7 g/cm^3) also increased the difficulties in milling.

Several countermeasures are being considered in our future research. Finer and more uniform powders would probably be

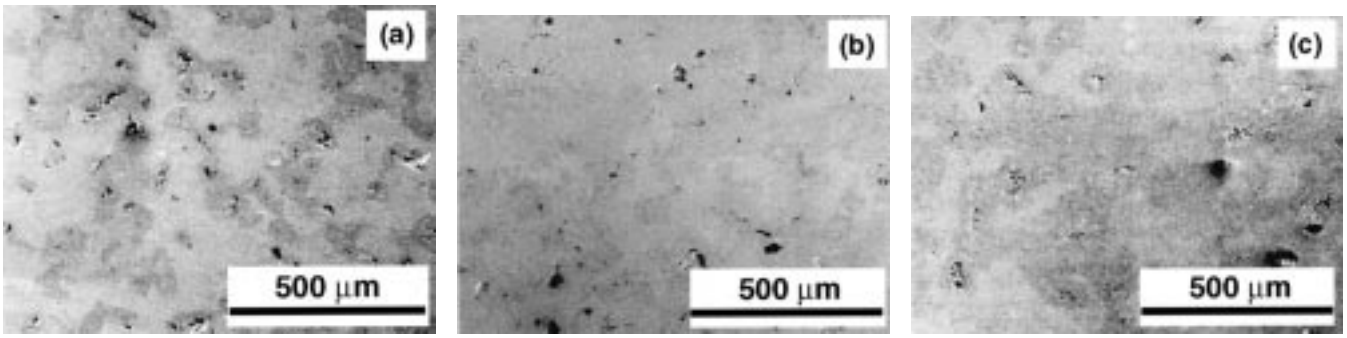

Fig. 6 Porosity morphologies of (**a**) Ir-25% Nb, (**b**) Ir-24% Nb-1% Al, and (**c**) Ir-25% Nb-1% Ni

Table 3 The phase, grain size, and porosities distribution of investigated samples

Alloy (at.%)	Phase in phase diagram	Phase after sintering	Grain size (μm)	Porosities distribution(a)
Ir-25% Nb	$L1_2$	$L1_2$ + fcc	<20	□ many; △ many
Ir-24% Nb-1% Al	$L1_2$	$L1_2$ + fcc + Nb	<20	□ many; △ many
Ir-25% Nb-1% Ni	$L1_2$	$L1_2$ + fcc	<20	□ many; △ more
Ir-50% Al	B2	B2 + fcc	~20	□ many
Ir-25% Ti	$L1_2$	$L1_2$ + Ti	5–40	□ a few; △ many

(a) △ small pore; and □ big pore

more effective and help solve some of the problems. Using a prealloyed powder of Ir-based refractory superalloys could bypass the milling problem and prevent metal loss as a result of solid-state diffusion. Of course, the sintering conditions are very important elements deserving further investigation.

4. Summary

The Ir-based refractory superalloys with a relative density greater than 90% theoretical density were obtained from elemental powders by the PECS method. Two phases were found among all the samples, although only a single phase was expected according to the phase diagrams. One reason is that the size of the powder particle is very different among each metal. Another reason is the milling problem.

The alloying process was progressed by prolonging the sintering time to 4 h, at which time, it was almost finished.

The predominant densification mechanisms are liquid-phase sintering for Ir-50 at.% Al and Ir- 25% Ti and solid-state diffusion for Ir-24% Nb-1% Al, Ir-25% Nb-1% Ni, and Ir-25 at.% Nb. Some improvements were made in pore elimination by introducing Al.

For PECS of Ir-based refractory superalloys, further study will be required.

Acknowledgments

The authors thank Drs. S. Nishimura and N. Hirosaki, for supplying the PECS equipment, and Dr. Y. Gu, for his valuable participation in related discussions.

References

1. D. Lupton and M. Hormann: *Galvanotechnik,* 1996, vol. 87 (1), pp. 72-80 (in German).
2. Y. Yamabe-Mitarai, Y. Ro, T. Maruko, and H. Harada: *Metall. Mater. Trans. A,* 1998, vol. 29A, pp. 537-49.
3. S.H. Yoo, T.S. Sudarshan, K. Sethuram, G. Subhash, and R.J. Dowding: *Powder Metallury,* 1999, vol. 42 (2), pp. 181-82.
4. Y. Yamabe-Mitarai and H. Harada: *ASM J. Mater. Eng. Performance,* in press.
5. D.E. Alman, N.S. Stoloff, and M. Otsuki: The Japan Institute of Metals, *JIMIS*-6, Sendai, Japan, 1991, pp. 891-99.
6. H. Hosoda, S. Watanabe, and S. Hanada: *MRS,* Boston, U.S.A., 1998, vol. 552, pp. KK8.33.1-KK8.33.7.
7. J.D. Bolton and A.J. Gant: *Powder Metall.,* 1997, vol. 40 (2), pp. 143-51.
8. J.R. Moon: *Powder Metall.,* 1989, vol. 32 (2), pp. 132-39.